NIH Public Access
Author Manuscript
J Invest Dermatol. Author manuscript; available in PMC 2012 January 1.

Published in final edited form as:
J Invest Dermatol. 2011 July ; 131(7): 1428–1434. doi:10.1038/jid.2011.61.

The *Samd9L* Gene: Transcriptional Regulation and Tissue-Specific Expression in Mouse Development

Qiujie Jiang[1], **Benjamin Quaynor**[1], **Alex Sun**[1], **Qiaoli Li**[1], **Hirotaka Matsui**[2], **Hiroaki Honda**[3], **Toshiya Inaba**[2], **Eli Sprecher**[4], and **Jouni Uitto**[4]

[1]Department of Dermatology and Cutaneous Biology, Jefferson Medical College, Philadelphia, PA

[2]Department of Molecular Oncology, Research Institute for Radiation Biology & Medicine, Hiroshima University, Hiroshima, Japan

[3]Department of Developmental Biology, Research Institute for Radiation Biology & Medicine, Hiroshima University, Hiroshima, Japan

[4]Department of Dermatology, Tel Aviv Sourasky Medical Center, Tel Aviv, Israel

Abstract

Normophosphatemic familial tumoral calcinosis (NFTC) is caused by mutations in the *SAMD9* gene. This gene is absent in mouse while there is a murine paralogue, *SamD9*-like (*Samd9L*). To clarify the relationships of *SAMD9* and *SAMD9L*, we investigated the transcriptional regulation and the expression pattern of mouse *Samd9L*. An ~1.5-kb mouse *Samd9L* promoter fragment was cloned, and a series of 5' deletion constructs were linked to a luciferase reporter gene. All constructs displayed significant activity in transfected epithelial cells and mouse fibroblasts, and the presence of regulatory *cis*-elements as close as 87 bp upstream of the transcription start site were identified. Ras-responsive element binding protein (Rreb-1) was identified in this region by protein-DNA binding array. The expression of *Samd9L* was up-regulated by calcitonin, and this was preceded by a significant increase in the expression of *Rreb-1* mRNA. qRT-PCR analysis of *Samd9L* revealed near-ubiquitous expression, with the highest level in the kidney. Tissue-specific expression was also confirmed both by *in situ* β-gal staining and quantitative enzymatic activity assay in a novel transgenic *Samd9L*$^{+/-}$ mouse in which the *LacZ* gene replaced exon 2 in the *Samd9L* gene. These findings assist in understanding the regulation of *Samd9L* in the context of its paralogous gene, *SAMD9*, which harbors mutations in NFTC.

Keywords

familial tumoral calcinosis; *Samd9L* gene expression; calcitonin regulation; Rasresponsive element binding protein

Introduction

Familial tumoral calcinosis (FTC; MIM610455) is a group of heritable disorders characterized by ectopic mineralization of extracellular matrix of connective tissues

*Address for Correspondence: Jouni Uitto, M.D., Ph.D., Department of Dermatology and Cutaneous Biology, Jefferson Medical College, 233 S. 10th Street, Suite 450 BLSB, Philadelphia, PA 19107, USA, Tel: (215) 503-5785, Fax: (215) 503-5788, Jouni.Uitto@jefferson.edu .

Conflict of Interest
The authors state no conflict of interest.

NIH-PA Author Manuscript
NIH-PA Author Manuscript
NIH-PA Author Manuscript

NIH-PA Author Manuscript

NIH-PA Author Manuscript

NIH-PA Author Manuscript

(Sprecher, 2010). The normophosphatemic variant, NFTC, manifests with extensive mineralization of cutaneous tissues, associated with inflammatory manifestations mostly evident in mucosal tissues. Recently, mutations in NFTC have been demonstrated in Sterile Alpha Motif Domain-containing 9 gene (*SAMD9*), which encodes a cytoplasmic protein with currently unknown function (Chefetz *et al*, 2000; Topaz *et al*, 2006). The *SAMD9* gene is located on human chromosome 7q21 region, and next to it in head-to-tail orientation is a paralogous gene, *SAMD9*-like (*SAMD9L*), both with similar structures in that there is one large, ~5–6 kb coding exon which is preceded upstream by a large intron and either one (*SAMD9L*) or several (*SAMD9*) relatively small non-coding exons (Li *et al*, 2007). Both human genes encode a putative protein of ~170–190 kb with 58% sequence homology, which in their amino terminal segments display a well conserved sterile alpha motif (SAM) domain potentially involved in protein/protein interactions.

In a recent study, gene expression differences were noted between cell cultures derived from an aggressive fibromatosis tumor as compared to control tissue (Li *et al*, 2007). In particular, reduced *SAMD9* expression was noted in aggressive fibromatosis, as well as in 20% of cases of breast cancer and 35% of cases of colon cancer cell lines compared to normal tissues. Thus, SAMD9 may play a role in regulating cell proliferation and suppressing the neoplastic phenotype. Recently, a common microdeletion cluster in the 7q21.3 subband region has been identified in patients with myeloid leukemia and myelodysplastic syndrome (Asou *et al*, 2009). This microdeletion region contains three genes, *SMAD9*, *SAMD9L*, and *Miki*, which were postulated as candidates for myeloid tumor suppressor genes on 7q. Finally, SAMD9 has been suggested to be a key molecule to control cancer cell death in malignant glioma by Sendai virus particle or interferon-β treatment (Tanaka *et al*, 2010). With respect to ectopic mineralization, it was noted that the NFTC patients generally develop calcium deposits in areas subject to repeated trauma and associated with marked inflammatory manifestations, suggesting that *SAMD9* may also play a role in the inflammatory response to tissue injury. It has been speculated that TNF-α, a proinflammatory cytokine that links inflammation and apotosis, might have a role in *SAMD9* regulation (Sprecher, 2010). Besides these observations, the physiological roles of *SAMD9* and *SAMD9L* are poorly understood.

An intriguing observation is that while an orthologous gene of human *SAMD9* exists in rat, the corresponding gene is lost in mouse lineage due to a unique genomic rearrangement (Li *et al*, 2007). However, mice do have the orthologue to human *SAMD9L* but very little is known of the regulation of the *Samd9*/*Samd9L* gene-gene system either in human or mouse. In this study, we have specifically explored the spatial and temporal expression of the *Samd9L* gene during mouse development as well as in a novel mouse “knockout” model in which part of the *Samd9L* coding region has been replaced by the *LacZ* gene.

Results and Discussion

To gain insight into the tissue-specific expression of *Samd9L*, a multiple mouse tissue panel was first screened for the corresponding mRNA by quantitative RT-PCR. The results indicated high level of expression in kidney, followed by spleen, stomach and adrenal gland, when the level of expression was normalized for mouse actin mRNA in the same samples (Fig. 1a). This near-ubiquitous expression of mouse *Samd9L* is consistent with previous findings by Li *et al* (2007) and Topaz *et al* (2006) who demonstrated that *SAMD9* and *SAMD9L* are expressed in all human adult, fetal and tumor tissues that were available from human multiple tissue cDNA panels. During mouse embryonic development at days 8.5 and 9.5, essentially no expression was detected (Fig. 1a, lanes 17 and 18), but low levels were detectable at days 12.5 and 19 (Fig. 1a, lanes 19 and 20). RT-PCR of mouse kidney revealed low, yet detectable levels of *Samd9L* mRNA at birth, and the expression levels significantly

NIH-PA Author Manuscript

NIH-PA Author Manuscript

NIH-PA Author Manuscript

increased during the subsequent 2 and 4 weeks of life (Fig. 1b, c). Computerized scanning analysis indicated that no further change in the *Samd9L* mRNA levels in mouse kidney was noted between 4 and 40 weeks of life (Fig. 1c).

To examine the transcriptional control of *Samd9L* gene expression, an expression construct extending from −1,428 to +98 was developed, and a number of 5'-deletion constructs were generated and linked to firefly luciferase (Luc) reporter (Fig. 2a). Transfection of four cell lines, including three epithelial cells and a mouse fibroblast cell line (NIH3T3), in culture with these reporter plasmids showed significant level of expression over controls mock transfected with the basic vector (Fig. 2b). The activity in epithelial cell cultures (TCMK-1, MLE-10 and HEK293) revealed that the shortest construct tested, p-87-Luc, showed the highest level of expression. Inclusion of upstream sequences up to −1,428 resulted in reduction of the activity suggesting the presence of down regulatory elements. In all cultures, co-transfection of a β-galactosidase expression plasmid (pRSV-β-gal) was included, followed by β-galactosidase enzyme activity determination which was used to correct for transfection efficiencies. The mouse fibroblast cell line (NIH3T3) showed reduced activity by about 50% with the p-87 construct as compared to other constructs tested containing the upstream sequences (Fig. 2b, lower right panel). It appears, therefore, that the proximal promoter region within the segment −87 to +98 contains the essential sequences necessary for high level of expression particularly in epithelial cell cultures.

Searching for transcription factors that might regulate the expression of the *Samd9L* promoter within the p-87 promoter fragment, nuclear extracts of NIH3T3 cells were tested in a protein/DNA filter array containing 96 transcription factors. A number of transcription factors were identified to bind to the target sequence in p-87, however, search for consensus sequences within the p-87 identified the corresponding cognate binding sites for only two of them, E47 and Rreb (Figs. 3a, b). E47 is widely expressed and binds specifically to the immunoglobulin κ-chain enhancer κE2. It shows homology with other proteins with a Helix-Loop-Helix dimerization domain signature of the MYC type. E47 has been reported to be essential for normal B-cell hematopoiesis (Frasca *et al*, 2003). RREB is a zinc finger transcription factor that binds to RAS-responsive elements (RREs) of gene promoters (Zhang *et al*, 2003). It has been shown that the calcitonin gene promoter contains an RRE and that RREB-1 binds to it and increases expression of calcitonin (Flajollet *et al*, 2009; Mukhopadhyay *et al*, 2007).

Since RREB has been suggested to be responsive to calcitonin, we tested the possibility that *Samd9L* gene expression might be mediated by calcitonin through Rreb, one of the transcription factors shown to bind to the proximal −87 promoter sequence. Incubation of NIH3T3 cells with calcitonin showed over 3-fold increase in *Samd9L* gene expression which was statistically significant at 4 and 7 days of incubation (Fig. 4a). Parallel assay of Rreb mRNA levels by RT-PCR revealed a statistical increase as early as at 24 hour point (Fig. 4b).

To demonstrate the specificity of the Rreb binding to the promoter activity, transient cell transfections with the wild-type (WT) p-87 plasmid reporter construct together with three mutant constructs in which segments of the consensus binding site of Rreb (−63/−49) were mutated (Fig. 5a). The WT construct showed over 4-fold level of expression of the luciferase reporter gene as compared to the control plasmid (Fig. 5b). No change was noted with Mutant 1, while Mutant 2 showed ~3-fold increase over the WT activity. Mutant 3 essentially abolished the promoter activity (Fig. 5b). Interestingly, the Mutant 2 also mutates the consensus binding site of SRY, a testis determining factor, which has been reported recently to also play a role in hormonal influence on calcification (Yamada *et al*, 2006).

NIH-PA Author Manuscript

NIH-PA Author Manuscript

NIH-PA Author Manuscript

Further studies, such as investigating gender differences in *SAMD9L* expression, are needed to understand the role of androgens in these processes.

The tissue-specific expression of the *Samd9L* promoter was also assessed in *in vivo* situations by examination of a heterozygous transgenic mouse in which exon 2 of the gene was replaced by *LacZ* gene *(SamD9L$^{+/-}$)*, and therefore the expression of β-galactosidase was under the *Samd9L* upstream regulatory sequences within the promoter. It should be noted that these *SamD9L$^{+/-}$* mice, as well as their homozygous counterparts, develop acute myelogenous leukemia at high frequency after they reach the age of 20 months. This mouse model has been preliminarily reported (Matsui *et al*, 2009), and a detailed manuscript is in preparation (Matsui et al., unpublished). Dissection of different tissues in *SamD9L$^{+/-}$* mice followed by β-galactosidase staining, confirmed the highest levels of expression in the kidney and spleen, while the level of expession was very low in the liver and the muscle (Fig. 6a). Histochemical staining of paraffin embedded sections for β-galactosidase revealed expression in both proximal and distal tubules (Fig. 6b). The localization of Samd9L protein in mouse kidney was further confirmed by immunohistochemical staining of paraffin sections of wild-type mouse kidney with a Samd9L primary antibody which revealed expression in tubules, but not in the glomeruli (Fig. 6c).

The expression of β-galactosidase was also quantitatively measured by enzymatic activity assay in the extracts from the same tissues that were stained for β-gal *in situ* (Fig. 6d). Highest level of enzymatic activity, as determined spectrophotometrically at 570 nm, after deduction of the background reflecting endogenous β-galactosidase activity, showed that the highest levels were observed in the kidney and the spleen confirming the results obtained by RT-PCR at the level of mRNA expression, as shown in Fig. 1a, and by β-galactosidase staining *in situ* (Fig. 6a).

In summary, the present study of mouse *Samd9L* revealed near-ubiquitous expression, with the highest level in the kidney, a major organ regulating calcium-phosphate homeostasis and the site of calcitonin hormonal action. The transcriptional regulation of *Samd9L* as explored in this study, adds to our understanding of the potential role of this gene in carcinogenesis. This information, in the context of the regulation of the SAMD9 gene expression, may contribute to our understanding of mineralization processes, such as those taking place in NFTC.

Materials and Methods

Animals

The *Samd9L* “knockout” mouse model was developed by homologous recombination resulting in replacement of exon 2 in the *Samd9L* gene by the *LacZ* gene (Matsui *et al*, 2009). C57/BL6 mice were from Jackson Labs (Bar Harbor, ME). All animal studies were performed in accordance with the Institutional guidelines of Thomas Jefferson University Animal Care and Use Committee and the National Institutes of Health. Mice were placed in cages in a temperature-controlled room with a 12-hr light-dark cycle and free access to food and water.

Cell Culture

All cell lines (NIH3T3, mouse skin fibroblasts; HEK293, human embryonic kidney epithelial cells; MLE-10, mouse liver epithelial cells; and TCMK-1, mouse kidney epithelial cells) were cultured in Dulbecco’s modified Eagle’s medium and supplemented with 10% heat-inactivated fetal bovine serum, 2 mM L-glutamine, 100 IU/ml penicillin, and 100 μg/ml streptomycin (Cellgro, Mediatech, Inc., Herndon, VA). Cultures were maintained at 37°C in a humidified atmosphere of 5% CO2 and 95% air.

NIH-PA Author Manuscript

NIH-PA Author Manuscript

NIH-PA Author Manuscript

Antibodies

Antibodies to mouse *Samd9L* were raised in rabbits to the peptide WPENKELDEDSTLIEC (Abgent, San Diego, CA). 4'-6-Diamidino-2-phenylindole (DAPI) was purchased from Invitrogen (Eugene, OR).

Immunofluorescence

Whole mouse kidney was embedded in paraffin and cut into 8 μm sections onto slides. The slides were then deparaffinized, permeabilized, and stained with anti-mouse Samd9L antibody at a 1:500 dilution followed by Texas Red secondary (red) antibody at a 1:300 dilution and counterstained with DAPI (blue) at a 1:5000 dilution, or only stained with Texas Red secondary antibody at a 1:300 dilution and counterstained with DAPI to serve as a control.

Promoter Plasmid Constructs

The serially truncated *Samd9L* promoter fragments with their 5'-ends ranging from −1428 to −87 and their 3'-end being fixed at +98, were prepared by PCR amplification of mouse genomic DNA using sense primers containing a *Mlu*I restriction site, and all of the constructs shared the same antisense primer containing a *Nhe*I restriction site (Table S1). The PCR products were separated by gel electrophoresis and extracted from a gel slice (Qiagen, Valencia, CA), then cloned into pCR-Blunt II-TOPO vector using ZeroBlunt TOPO PCR Cloning kit (Invitrogen, Carlsbad, CA). The plasmid was then digested with *Mlu*I and *Nhe*I and cloned into pGL3-Basic luciferase vector (Promega, Madison, WI). Mutagenesis of the Rreb-binding site in the p-87 reporter construct, spanning from −87 to +98, was performed by site-directed mutagenesis using the QuikChange XL Site-Directed Mutagenesis kit (Stratagene, La Jolla, CA) and the manufacturer's instructions with specific primers. The final constructs were sequenced in both directions to ensure correct nucleotide sequence. Computer analysis of the promoter region of *Samd9L* was conducted to detect putative *cis*-acting elements using a transcription factor database (TFSEARCH, Kyoto University, version 1.3).

Transient Transfections and Luciferase Assay

Plasmid constructs used for transient transfection were prepared using a purification kit (Qiagen). All cell lines (NIH3T3, HEK293, MLE-10, TCMK-1) were plated on a 24-well plate 24 hours prior to transfection and grown to approximately 80% confluency. The cells in each well were cotransfected with 0.75 μg of experimental plasmid and 0.25 μg of pRSV-β-galactosidase expression plasmid as an internal control for transfection efficiency, using FuGENE6 transfection reagent according to the manufacturer's instructions (Roche Diagnostic Co., Indianapolis, IN). After incubation for 50 hours, the transfected cells were harvested and assayed as previously described. Each experiment was performed in triplicate.

Quantitative Expression of mRNA in Mouse Tissues

RapidScan gene expression cDNA arrays containing mouse tissues for quantitative PCR were purchased from OriGene (Rockville, MD). These arrays contained prestandardized amounts of cDNA from 20 independent mouse tissues. The cDNA was amplified by PCR using primers specific for *Samd9L* (sense, located in exon 1: 5'-CCTGGTGTCTCTCAGCCAGT-3'; antisense, located in exon 2: 5'-CTTCATTCTGCCCTGTCTCC-3'). PCR products were separated by gel electrophoresis on a 2% agarose gel and stained with ethidium bromide.

NIH-PA Author Manuscript

NIH-PA Author Manuscript

NIH-PA Author Manuscript

RNA Extraction and Reverse Transcription-PCR

NIH3T3 cells were plated on 100 mm dishes 24 hours prior to treatment and allowed to grow to 60% confluence. The cells were then washed with PBS and incubated with media containing 200 ng/L calcitonin (American Peptide Company, Sunnyvale, CA) for the indicated time period. Total RNA was extracted from NIH3T3 cells using an RNeasy Mini Kit (Qiagen, Valencia, CA) following the manufacturer's instructions. Total RNA was treated with DNase I to eliminate amplification of genomic DNA. The amount and quality of RNA were verified by measuring the absorbance at 260/280 nm. Random-primed reverse transcription of RNA was performed with the Superscript First-Strand Synthesis System for RT-PCR (Invitrogen).

SYBR Green PCR amplification was performed in a model 7000 sequence detector (Applied Biosystems, Foster City, CA). The reactions were carried out in a 96-well plate in a 25 μl reaction volume containing 12.5 μl of 2× SYBR Green PCR Master Mix (Applied Biosystems), 0.3 nM concentrations of forward and reverse primers each, and 10 ng of cDNA. Initial incubation at 95°C for 15 min was followed by 40 cycles of 95°C for 15 seconds and either 56°C (for *Samd9L*) or 60°C (for *Rreb*) for 1 min. NIH3T3 cDNA samples in triplicate were used in each run. The amount of specific mRNA in each RNA sample was quantified and normalized to *Gapdh* mRNA. The relative expression level of the target genes was calculated using the ΔΔCt method (Real-time PCR software; model 7000 sequence detector; Applied Biosystems). Reaction specificity was determined by the dissociation curve immediately after the last reaction cycle, and visualized with the software Dissociation Curve 1.0 (7000 sequence detection system; Applied Biosystems).

Protein/DNA array

A 187-bp fragment of the *Samd9L* promoter region, extending from −87 to +98, was excised from the p-87 construct with restriction enzymes *Mlu*I and *Nhe*I, and labeled with biotin using Bio-16-dUTP (Roche, Mannheim, Germany) and the Klenow fragment of DNA polymerase I (Invitrogen). Unincorporated Bio-16-dUTP was removed by a spin column and the biotin-labeled DNA fragment was coupled to M-280 streptavidin magnetic beads (Dynal Biotech, Oslo, Norway) using the manufacturer's conditions. The DNA-coupled magnetic beads were incubated with 500 μg protein from NIH3T3 nuclear extract for 2 hours at 4°C in the binding buffer as previously described. After washing, the bound proteins were dissociated from the DNA-coupled beads by incubating in a buffer containing 2 M NaCl for 60 minutes on ice. The bound proteins extracted from the 187-bp promoter region fragment were incubated with the TranSignal (Panomics, Redwood, CA) probe mix, a set of 96 biotin-labeled DNA oligonucleotides corresponding to the consensus sequences for the corresponding transcription factors to allow the formation of DNA/protein complexes. The transcription-factor bound probes were isolated and then dissociated from the DNA/protein complex and used to hybridize the TranSignal Array spotted with complementary consensus-binding sequences of the transcription factor probes according to manufacturer's instructions. Hybridization signals were visible after exposure to X-ray film following chemiluminescent detection.

β-Gal Staining and Quantitative Enzymatic Activity Assay

To analyze the biodistribution and expression of the mouse Samd9L, various tissues were isolated from adult *Samd9L*$^{-/-}$ mice and examined for beta-galactosidase expression *in vivo*. The tissues fixed with 4% paraformaldehyde were stained for β-galactosidase using a LacZ Detection kit (InvivoGen, San Diego, CA). The sections were lightly counterstained with neutral red before mounting. For the enzyme activity assays, the various tissues were harvested from either *Samd9L*$^{+/-}$ mice or wild-type mice, and tissue extracts were analyzed for beta-galactosidase using a β-gal assay kit (Invitrogen) (Payet *et al*, 1998). The beta-

NIH-PA Author Manuscript

NIH-PA Author Manuscript

NIH-PA Author Manuscript

galactosidase activity in each tissue from wild-type mice was used as the baseline. The data were expressed after normalization to the corresponding baselines and to the protein content in each extract.

Statistical Analysis

Statistical differences between the means in various groups were calculated by Student's two-tailed *t*-test.

Supplementary Material

Refer to Web version on PubMed Central for supplementary material.

Abbreviations

Samd9L	sterile alpha motif domain-containing 9-like
NFTC	normophosphatemic familial tumoral calcinosis
Rreb1	Ras-responsive element binding protein 1

Acknowledgments

The authors thank Alix Grand-Pierre and Carol Kelly for assistance. This study was supported by DHHS, NIH/NIAMS grants R01 AR28450 (JU) and K08 AR057099 (QJ). Qiaoli Li is recipient of a Dermatology Foundation Research Career Development Award.

References

Asou H, Matsui H, Ozaki Y, et al. Identification of a common microdeletion cluster in 7q21.3 subband among patients with myeloid leukemia and myelodysplastic syndrome. Biochem Biophys Res Commun. 2009; 383:245–251. [PubMed: 19358830]

Chefetz I, Ben Amitai D, Browning S, et al. Normophosphatemic familial tumoral calcinosis is caused by deleterious mutations in SAMD9, encoding a TNF-alpha responsive protein. J Invest Dermatol. 2008; 128:1423–1429. [PubMed: 18094730]

Flajollet S, Poras I, Carosella ED, et al. RREB-1 is a transcriptional repressor of HLA-G. J Immunol. 2009; 183:6948–6959. [PubMed: 19890057]

Frasca D, Nguyen D, Riley RL, et al. Decreased E12 and/or E47 transcription factor activity in the bone marrow as well as in the spleen of aged mice. J Immunol. 2003; 170:719–726. [PubMed: 12517933]

Li CF, MacDonald JR, Wei RW, et al. Human sterile alpha motif domain 9, a novel gene identified as down-regulated in aggressive fibromatosis, is absent in the mouse. BMC Genomics. 2007; 8:92–109. [PubMed: 17407603]

Matsui, H.; Nagamachi, A.; Ozaki, Y., et al. Loss of *Titan* (*Samd9L*), a candidate -7/9q- responsible gene encoding an actin remodeling regulator, develops MDS/AML in cooperation with *Evi1* or *Fbx/10*; ASH Annual Meeting and Exposition; New Orleans, LA, USA. 2009. Abstr. 2963

Mukhopadhyay NK, Cinar B, Mukhopadhyay L, et al. The zinc finger protein ras-responsive element binding protein-1 is a coregulator of the androgen receptor: implications for the role of the Ras pathway in enhancing androgenic signaling in prostate cancer. Mol Endocrinol. 2007; 21:2056–2070. [PubMed: 17550981]

Payet V, Arnauld C, Picault JP, et al. Transcriptional organization of the avian adenovirus CELO. J Virol. 1998; 72:9278–9285. [PubMed: 9765475]

Sprecher E. Familial tumoral calcinosis: from characterization of a rare phenotype to the pathogenesis of ectopic calcification. J Invest Dermatol. 2010; 130:652–660. [PubMed: 19865099]

NIH-PA Author Manuscript

NIH-PA Author Manuscript

NIH-PA Author Manuscript

Tanaka M, Shimbo T, Kikuchi Y, et al. Sterile alpha motif containing domain 9 is involved in death signaling of malignant glioma treated with inactivated Sendai virus particle (HVJ-E) or type I interferon. Int J Cancer. 2010; 126:1982–1991. [PubMed: 19830690]

Thiagalingam A, De Bustros A, Borges M, et al. RREB-1, a novel zinc finger protein, is involved in the differentiation response to Ras in human medullary thyroid carcinomas. Mol Cell Biol. 1996; 16:5335–5345. [PubMed: 8816445]

Topaz O, Indelman M, Chefetz I, et al. A deleterious mutation in SAMD9 causes normophosphatemic familial tumoral calcinosis. Am J Hum Genet. 2006; 79:759–765. [PubMed: 16960814]

Yamada T, Hirotaka K, Koshizuka Y, et al. Carminerin contributes to chondrocyte calcification during endochondral ossification. Nat Med. 2006; 12:665–670. [PubMed: 16680148]

Zhang S, Xiaolan Q, Chanelle R, et al. $p16^{INK4a}$ gene promoter variation and differential binding of a repressor, the ras-responsive zinc-finger transcription factor, RREB. Oncogene. 2003; 22:2285–2295. [PubMed: 12700664]

NIH-PA Author Manuscript

NIH-PA Author Manuscript

NIH-PA Author Manuscript

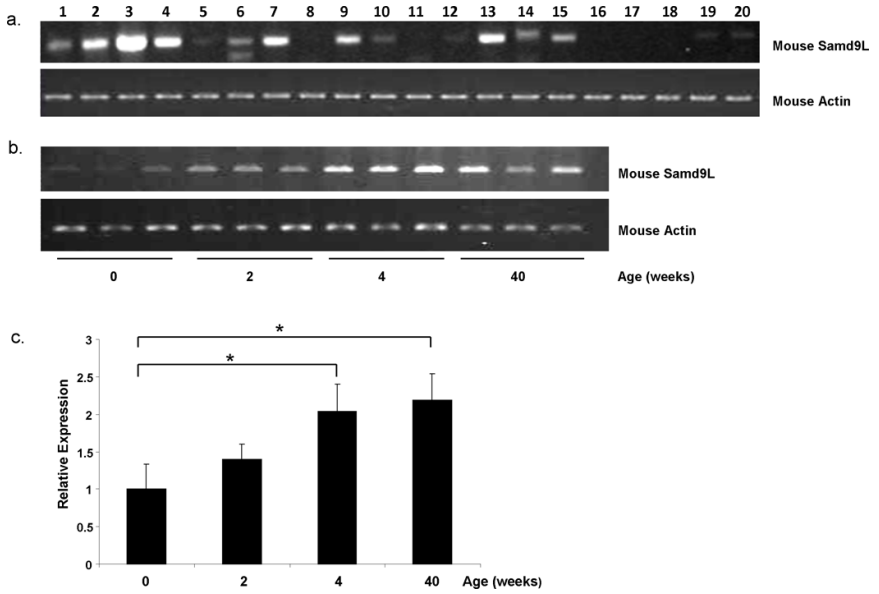

Figure 1. *Samd9L* expression is tissue-specific and developmentally regulated

(a) *Samd9L* mRNA expression was assessed by PCR using a pre-standardized cDNA library of multiple mouse tissues. The represented tissues are as follows: 1. Brain; 2. Heart; 3. Kidney; 4. Spleen; 5. Thymus; 6. Liver; 7. Stomach; 8. Small Intestine; 9. Muscle; 10. Lung; 11. Testis; 12. Skin; 13. Adrenal Gland; 14. Pancreas; 15. Uterus; 16. Prostate Gland; 17. Embryo/8.5 day; 18. Embryo/9.5 day; 19. Embryo/12.5 day; 20. Embryo/19 day. (b) The kidneys were harvested from the mice at the different ages. RT-PCR analysis revealed that the expression of mouse *Samd9L* in the kidneys increased with age when the mice at the age of 0 (newborn), 2, 4 and 40 weeks were examined. (c) The levels of *Samd9L* mRNA expression were quantified by determining the pixel intensities of the bands of RT-PCR products on the images in (b) using a computer program (ImageQuant, Molecular Dynamics, Sunnyvale, CA), and normalized with those of the corresponding internal actin controls. Data from three independent measurements were used (mean ± SD). The relative expression of mouse *Samd9L* was calculated using the mRNA level of mouse *Samd9L* in the newborns as 1 (*$p < 0.05$).

NIH-PA Author Manuscript

NIH-PA Author Manuscript

NIH-PA Author Manuscript

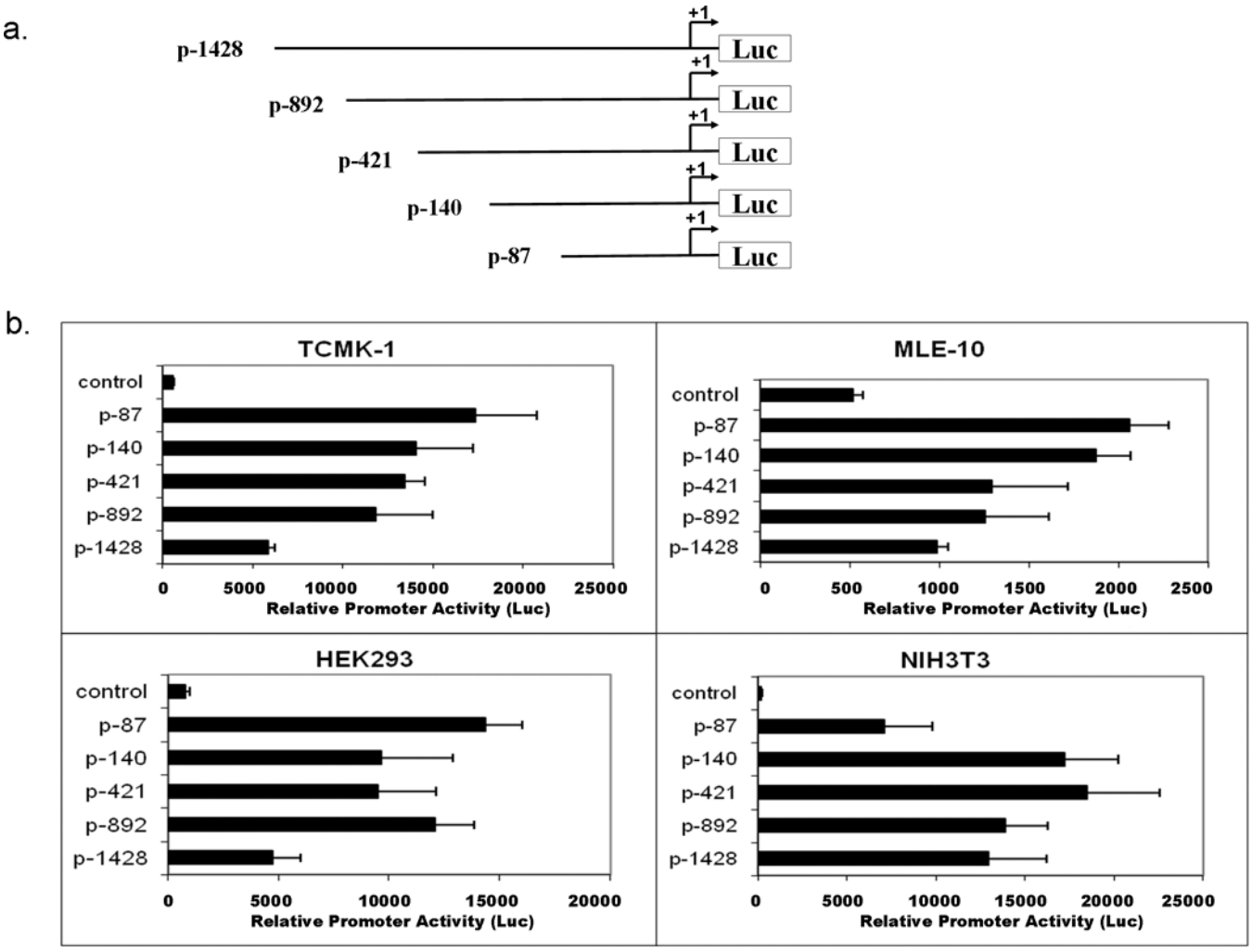

Figure 2. Serially truncated 5' deletion constructs of the mouse *Samd9L* promoter display significant activities in various cell lines

(a) Serial deletion constructs of the mouse *Samd9L* 5'- flanking region were inserted upstream of firefly luciferase gene (Luc) in the reporter plasmid pGL3-Basic. The numbers on the left indicate the 5' position of the construct, starting from the transcription start site (+1; arrow). (b) The *Samd9L* promoter constructs (0.75 μg) described in (a) or the control pGL3-Basic vector were cotransfected with 0.25 μg of pRSV-β-galactosidase reporter plasmid into the indicated cell types using FuGENE6 reagent (Roche). The cells were lysed 50 hours later and assayed for luciferase and β-galactosidase activities. Luciferase activity was divided by β-galactosidase activity to correct for transfection efficiency. The data are presented as the mean ± SD of three separate experiments each performed in triplicate. TCMK-1, mouse kidney epithelial cell line; MLE-10, mouse liver epithelial cell line; HEK293, human embryonic kidney epithelial cell line; NIH3T3, mouse skin fibroblast cell line.

NIH-PA Author Manuscript

NIH-PA Author Manuscript

NIH-PA Author Manuscript

a.

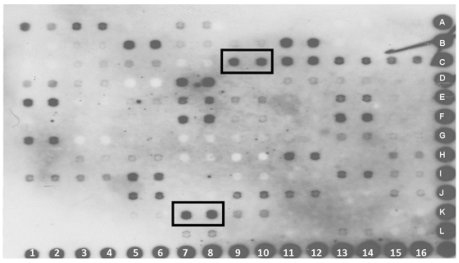

c.

-87-AGGTCTTTGGGTTTTACCCAAACAAACCAGCAGGTGGCATAGTTGGCACTAAA
----------RREB
----------SRY
---------- E47
+1
GAGCAGAAAAAGAGAAAAAAAGCATTTCAGGAAGTCTCTTTCTGTATCAGAA
----------HNF-3b
---------- c-Ets-
TCGAAACTGGAAACTGAAGCAGAGGTGGTTTTTTACTTCCTTACACTCTTGCCA
GCATTAGCCACACC -+98

b.

ADR1	ADR1	AhR/ Arnt	AhR/ Arnt	ANG-IRE	ANG-IRE	Antiox. RE	Antiox. RE	AP3	AP3	AP4 (RIP60)	AP4 (RIP60)	β-resp. element	β-resp. element	CdxA/ NKX2	CdxA/ NKX2	A
CEF1	CEF1	CEF2	CEF2	CETF/ CRE	CETF/ CRE	COUP-TF	COUP-TF	CREB-BP1	CREB-BP1	c-Rel	c-Rel	DR-9	DR-9	DR-1	DR-1	B
DR-2	DR-2	DR-3	DR-3	DR-4	DR-4	DR-5	DR-5	E47	E47	E4BP4	E4BP4	E4F, ATF	E4F, ATF	Elk1	Elk1	C
EVI-1	EVI-1	FKHR (human)	FKHR (human)	Fkhr (mouse)	Fkhr (mouse)	Afxh (Foxo4)	Afxh (Foxo4)	Freac-2 (1)	Freac-2 (1)	Freac-2 (2)	Freac-2 (2)	Freac-4	Freac-4	Freac-7	Freac-7	D
GAG	GAG	GAS	GAS	GATA-1	GATA-1	GATA-1/2	GATA-1/2	GATA-2	GATA-2	GATA-3	GATA-3	GATA-4	GATA-4	GATA-6	GATA-6	E
Gfi-1	Gfi-1	HAS	HAS	HBS	HBS	HBS + HAS	HBS + HAS	HFH-1	HFH-1	HFH-2	HFH-2	HFH-3	HFH-3	HFH-8	HFH-8	F
HIF-1	HIF-1	HNF-3	HNF-3	HNF-3β	HNF-3β	HNF-4	HNF-4	HNF-4/COUP-TF	HNF-4/COUP-TF	Ikaros5	Ikaros	IRF-1/2	IRF-1/2	ISRE(1)	ISRE(1)	G
ISRE(2)	ISRE(2)	ISRE (TransTF)	ISRE (TransTF)	L-III BP	L-III BP	KKLF	KKLF	MEF-2(1)	MEF-2(1)	MEF-2(2)	MEF-2(2)	MEF-3	MEF-3	MSP1	MSP1	H
MT-Box	MT-Box	MUSF1	MUSF1	MZF1	MZF1	NF-Y	NF-Y	Nkx-2.5	Nkx-2.5	NPAS2	NPAS2	HBS/ xbp-1	HBS/ xbp-1	NZF-3	NZF-3	I
ORE	ORE	p300	p300	PARP	PARP	Pax2	Pax2	Pax3	Pax3	Pax4	Pax4	Pax6	Pax6	Pax8	Pax8	J
PPARa	PPARa	PPARr	PPARr	RREB(1)	RREB(1)	RREB (2)	RREB (2)	RSRFC4	RSRFC4	SAA	SAA	Skn	Skn	SRY	SRY	K
Tax/ CREB	Tax/ CREB	TCF/LEF	TCF/LEF	XBP-1	XBP-1	XRE	XRE	ZIA	ZIA	ZIB	ZIB	ZIC	ZIC	ZID	ZID	L
1	2	3	4	5	6	7	8	9	10	11	12	13	14	15	16	

Figure 3. Protein/DNA array identifies select transcription factors binding to the mouse *Samd9L* promoter region

(a) Hybridization signals of the transcription factors bound to the p-87 promoter fragment identified in nuclear extracts of NIH3T3 cells. The TranSignal protein/DNA filter contains 96 transcription factors, each tested in duplicate (adjacent horizontal dots). (b) The transcription factors identified by the protein/DNA array as binding to *Samd9L* promoter region are indicated on shaded background. The selected transcription factors whose putative recognition sites that were identified by TFSEARCH (version 1.3, Kyoto University, Japan) in the p-87 promoter fragment are outlined by black frame in (a and b). Insufficient signal was noted for those factors shown on the white background. (c) The sequence extending from −87 to +98 was scanned for transcription factor-binding sites by using TFSEARCH. The putative recognition sites for select transcription factors identified in DNA are indicated below the sequence. The transcription initiation site is referred to by +1.

NIH-PA Author Manuscript

NIH-PA Author Manuscript

NIH-PA Author Manuscript

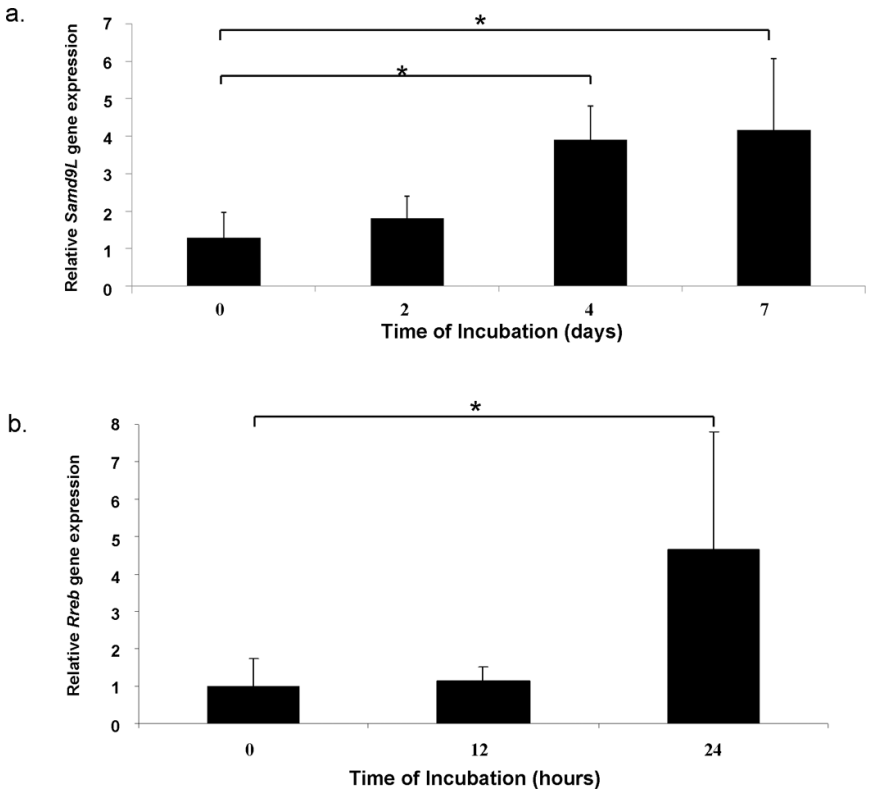

Figure 4. Calcitonin enhances the expression of mouse *Samd9L* and *Rreb* genes in NIH 3T3 cells *in vitro*

RT-PCR was performed using total RNA isolated from NIH3T3 cells cultured with 200 ng/L calcitonin for the indicated time periods using primers specific for *Samd9L*, *Rreb* and *Gapdh*, as described in Materials and Methods. The data were normalized to the *Gapdh* endogenous control and are presented as fold change as compared to untreated cells (0 time point). *Samd9L* expression is presented in the top panel (a) and *Rreb* expression in the bottom panel (b) Asterisks indicate statistical significance ($p < 0.05$) when compared to the corresponding controls.

NIH-PA Author Manuscript

NIH-PA Author Manuscript

NIH-PA Author Manuscript

a.

Consensus:	C	C	C	C	A	A	A	C	C	A	C	C	C	C
WT (-63/-49):	T	A	C	C	C	A	A	A	C	A	A	A	C	C
Mut1 (-63/-49):	-	T	T	T	-	-	-	-	-	-	-	-	-	-
Mut2 (-63/-49):	-	-	-	-	T	T	T	T	-	-	-	-	-	-
Mut3 (-63/-49):	-	-	-	-					-	T	T	T	T	-

b.

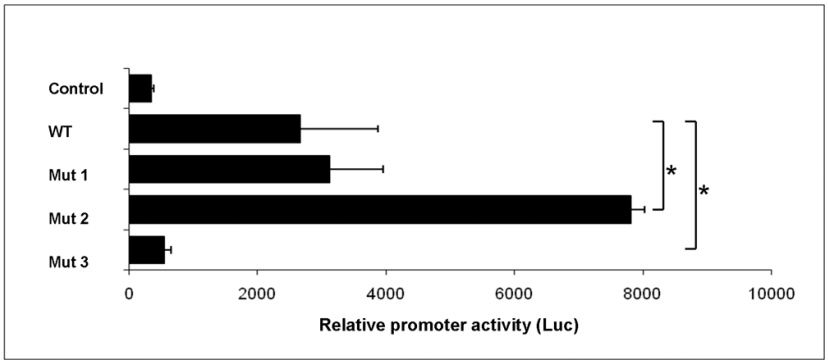

Figure 5. Mutations in the Rreb binding site sequences alter the activity of *Samd9L* gene promoter

(a) Sequences for the published (Thiagalingam *et al*, 1996) consensus sequence for the RREB binding site and WT sense strand of the p-87 plasmid construct (sequence homology boxed), as well as mutated plasmids (Mut 1, Mut 2, Mut 3) developed by site-directed mutagenesis with mutant primers, as described in Materials and Methods, are indicated in the figure. (b) The WT and mutant constructs were cotransfected with pRSV-β-galactosidase plasmid (0.75 μg to 0.25 μg, respectively) into NIH 3T3 cells using FuGENE6 (Roche), lysed after 50 hours of incubation, and then assayed for luciferase activity (Luc) which was normalized by β-galactosidase activity to correct for transfection efficiency. The data are presented as the mean ± SD of three independent experiments each performed in triplicate. Asterisks indicate statistical significance ($p < 0.05$) when compared to the WT construct.

NIH-PA Author Manuscript
NIH-PA Author Manuscript
NIH-PA Author Manuscript

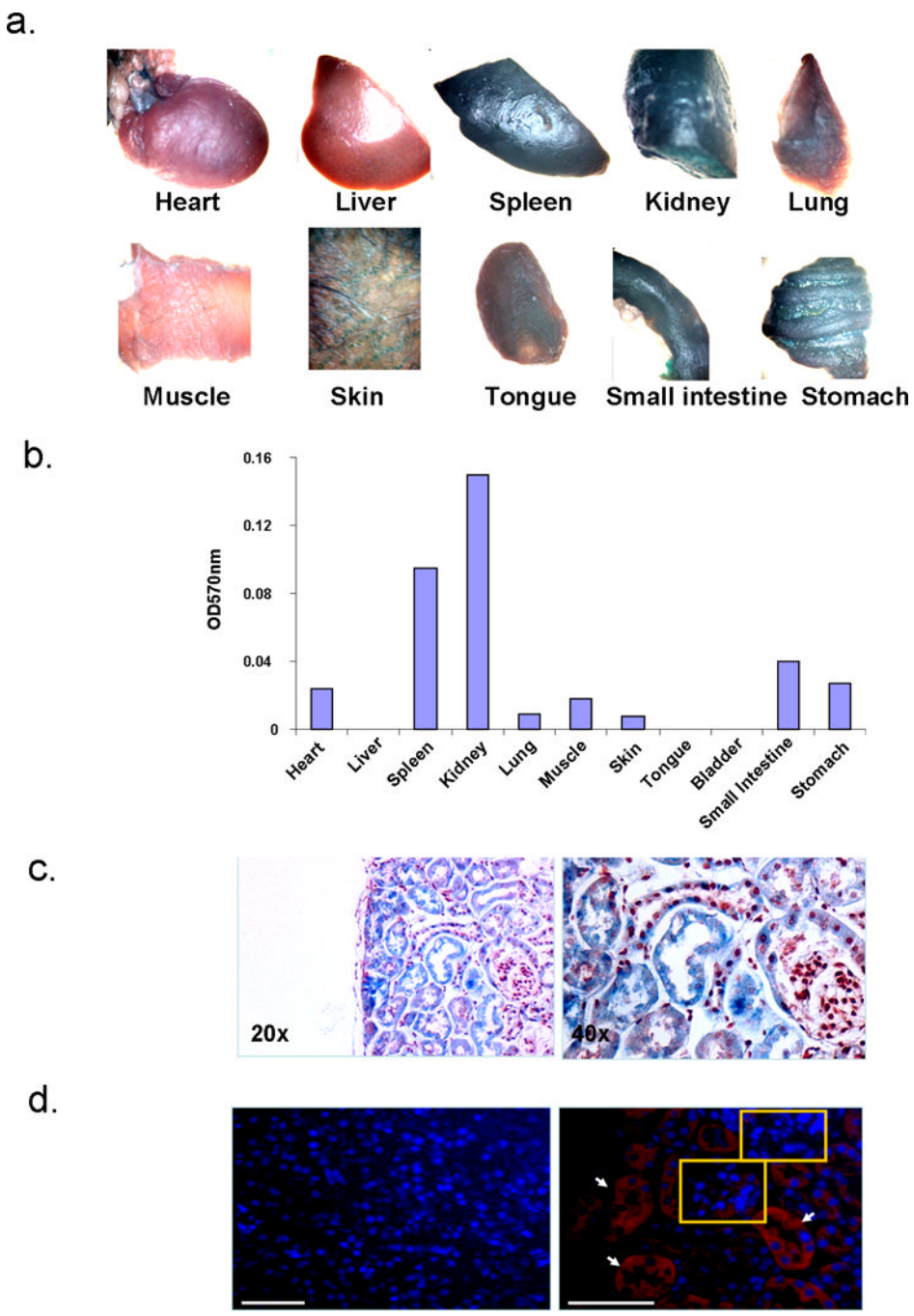

Figure 6. Assessment of *Samd9L* reveals tissue-specific expression *in vivo*

(a) Various organs were harvested from *Samd9L*$^{+/-}$ mice, in which the *LacZ* gene replaced exon 2 in the *Samd9L* gene in one allele, and were analyzed by in situ β-Gal staining. (b) Tissue-specific expression was analyzed by quantitative enzymatic activity assay in a transgenic *Samd9L*$^{+/-}$ mouse. The β-galactosidase activity in each tissue of the wild-type mice was used as the baseline, and the data were expressed after normalization to the corresponding baselines and to the protein content of each extract. The highest β-galactosidase enzymatic activity was observed in the kidney and spleen. (c) Paraffin sections of the β-Gal stained kidney confirmed localization in both proximal and distal tubules. (d) Paraffin sections of WT mouse kidney was stained with Samd9L primary antibody and

NIH-PA Author Manuscript

NIH-PA Author Manuscript

NIH-PA Author Manuscript

Texas Red secondary antibody and counter-stained with DAPI (right panel), or stained only with Texas Red secondary antibody and DAPI (left panel). The Samd9L was expressed in the tubules (arrows) but not in the glomerulis (in rectangles). Scale bar, 100 μm.